arXiv:0709.2774v1 [cond-mat.mtrl-sci] 18 Sep 2007

Intense terahertz laser fields on a two-dimensional hole gas with Rashba spin-orbit coupling

Y. Zhou

Hefei National Laboratory for Physical Sciences at Microscale and Department of Physics, University of Science and Technology of China, Hefei, Anhui, 230026, China

(Dated: February 1, 2008)

We investigate the influence on the density of states and the density of spin polarization for a two-dimensional hole gas with Rashba spin-orbit coupling under intense terahertz laser fields. Via Floquet theorem, we solve the time-dependent Schrödinger equation and calculate these densities. It is shown that a terahertz magnetic moment can be induced for low hole concentration. Different from the electron case, the induced magnetic moment is quite anisotropic due to the anisotropic spin-orbit coupling. Both the amplitude and the direction of the magnetic moment depend on the direction of the terahertz field. We further point out that for high hole concentration, the magnetic moment becomes very small due to the interference caused by the momentum dependence of the spin-orbit coupling. This effect also appears in two-dimensional electron systems.

PACS numbers: 71.70.Ej, 78.67.De, 73.21.Fg, 78.90.-t

Optical properties of semiconductors are sensitive to external conditions. Almost fifty years ago Franz[1] and Keldysh[2] pointed out that under static electric fields the absorption coefficient becomes finite below the band gap, and the above-gap absorption spectrum shows oscillations. In the late 1990s, Jauho and Johnsen[3,4] studied the optical properties of semiconductors under strong ac field and developed dynamic Franz-Keldysh effect (DFKE), which presents the blueshift of the main absorption edge and the fine structure near the band gap. This effect is particularly obvious for semiconductors under intense terahertz (THz) field, thereby leading to extensive theoretical and experimental interests on THz electro-optics.[5,6,7,8] Very recently Cheng and Wu brought the spin degrees of freedom into the study of the THz field induced effects. They studied a two-dimensional electron gas (2DEG) with the Rahhba spin-orbit coupling (SOC) under intense terahertz field.[9] It is shown that the THz field can efficiently modify the density of states (DOS) of the 2DEG and excite a magnetic moment oscillating at THz frequency. Later, Jiang et al. studied similar effects of quantum dots[10], and further discussed the spin dissipation under THz driving fields.[11] However, all these works concentrate on electron systems. Up to now there is no study on the spin properties of hole systems under intense THz field. In this letter we study the effect of intense terahertz laser fields on a two-dimensional hole gas (2DHG) with Rashba SOC and show that this system has some new properties different from the previously studied electron system.

We consider a p-type GaAs (100) quantum well (QW). The growth direction is denoted as the z axis. A uniform THz radiation field (RF) $\mathbf{E}_{\mathtt{THz}}(t) = \mathbf{E}\cos(\Omega t) = (E_x, E_y, 0)\cos(\Omega t)$ is applied in the x-y plane with the period $T_0 = 2\pi/\Omega$. The angle between the electric field and x axis is $\theta_{\mathbf{E}}$. By using the Coulomb gauge, the vector and scalar potentials can be written as $\mathbf{A}(t) = -\mathbf{E}\sin(\Omega t)/\Omega$ and $\phi(t) = 0$, respectively. We assume the well width is small enough so that only the lowest subband is relevant. For this structure, the lowest subband is heavy hole (HH) like. By applying a suitable strain, it can be light hole (LH) like. The confinement is assumed to be large enough so that the lowest HH and LH subbands are well separated and we can consider the HHs and LHs separately. The Hamiltonian can be written as ($\hbar \equiv 1$)

$$H_\lambda(\mathbf{K}, t) = \frac{\mathbf{K}^2}{2m^*_\lambda} + H^\lambda_{so}(\mathbf{K}, t) \ . \tag{1}$$

Here $\lambda = LH, HH$ and $\mathbf{K} = \mathbf{k} - e\mathbf{A}(t)$, with $\mathbf{k}$ standing for the electron momentum. m^*_λ is the effective mass. For GaAs QW, H_{so} is mainly due to the Rashba term,[12] and can be written as $H^\lambda_{so}(\mathbf{K}) = \frac{1}{2}(\sigma_x\Omega^\lambda_x + \sigma_y\Omega^\lambda_y)$. Here, σ is the Pauli matrix. For HHs, we have[13,14]

$$\Omega^{HH}_x(\mathbf{K}) = 2K_y(\gamma^{HH}_a K_y^2 + \gamma^{HH}_b K_x^2) \ , \tag{2}$$
$$\Omega^{HH}_y(\mathbf{K}) = 2K_x(\gamma^{HH}_a K_x^2 + \gamma^{HH}_b K_y^2) \ , \tag{3}$$

with $\gamma^{HH}_a = E_z(\gamma^{7h7h}_{53} + \gamma^{7h7h}_{54})$, $\gamma^{HH}_b = E_z(\gamma^{7h7h}_{53} - 3\gamma^{7h7h}_{54})$. For LHs,

$$\Omega^{LH}_x(\mathbf{K}) = 2K_y(\gamma^{LH}_a K_y^2 + \gamma^{LH}_b K_x^2 + \gamma^{LH}_c\langle k_z^2\rangle) \ , \tag{4}$$
$$\Omega^{LH}_y(\mathbf{K}) = -2K_x(\gamma^{LH}_a K_x^2 + \gamma^{LH}_b K_y^2 + \gamma^{LH}_c\langle k_z^2\rangle) \ , \tag{5}$$

with $\gamma^{LH}_a = E_z(\gamma^{6l6l}_{53} + \gamma^{6l6l}_{54})$, $\gamma^{LH}_b = E_z(\gamma^{6l6l}_{53} - 3\gamma^{6l6l}_{54})$, $\gamma^{LH}_c = E_z\gamma^{6l6l}_{52}$. It is noted from these equations that the magnitude of the Rashba term can be tuned by the external electric field E_z applied on the sample.[15,16] In Eqs. (2)-(5), γ^{7h7h}_{53}, γ^{7h7h}_{54}, γ^{6l6l}_{52}, γ^{6l6l}_{53}, γ^{6l6l}_{54} are the Rashba coefficients.[13] They depend both on the property of material and QW well width.

Similar to Refs. 9 and 10, by employing the Floquet theorem,[17] the solution of the Schrödinger equation with

time-dependent Hamiltonian $H_\lambda(\mathbf{K},t)$ can be written as

$$\Phi_s^\lambda(\mathbf{k},t) = e^{-i\{(E_{\mathbf{k}}^\lambda+E_{em}^\lambda)t-b_0\mathbf{k}\cdot\mathbf{E}[\cos(\Omega t)-1]-\gamma\sin(2\Omega t)\}} \times e^{-q_s^\lambda(\mathbf{k})t}\sum_{n=-\infty}^{\infty}\phi_{n,s}^\lambda(\mathbf{k})e^{in\Omega t} \quad (6)$$

Here $s=\pm$ represents the two helix spin branches; $E_{\mathbf{k}}^\lambda = \mathbf{k}^2/2m_\lambda^*$ is the kinetic energy of HHs or LHs; $E_{em}^\lambda = e^2E^2/(4m_\lambda^*\Omega^2)$ is the energy induced by the RF due to the DFKE; $b_0 = e/(m_\lambda^*\Omega^2)$; $\gamma = E_{em}/(2\Omega)$. $\phi_{n,s}^\lambda(\mathbf{k}) = (\phi_{n,s}^{\lambda,\sigma}(\mathbf{k})) \equiv \binom{\phi_{n,s}^{\lambda,+1}(\mathbf{k})}{\phi_{n,s}^{\lambda,-1}(\mathbf{k})}$ in Eq. (6) are the expansion coefficients of the Floquet states with $\sigma=1$ (-1) representing spin-up $\uparrow$ (-down $\downarrow$) in the laboratory coordinates (along the z axis). $q_s(\mathbf{k})$ is the corresponding eigenvalue and can be determined by

$$\begin{aligned}&[n\Omega - q_s^\lambda(\mathbf{k})]\phi_{n,s}^\sigma + \big\{[D_{01}^\lambda(\mathbf{k})\pm i\sigma D_{02}^\lambda(\mathbf{k})] + 2(e/2\Omega)^2[D_{21}^\lambda(\mathbf{k})\pm i\sigma D_{22}^\lambda(\mathbf{k})]\big\}\phi_{n,s}^{-\sigma}\\ &+\big\{i(e/2\Omega)[D_{11}^\lambda(\mathbf{k})\pm i\sigma D_{12}^\lambda(\mathbf{k})] + 3i(e/2\Omega)^3[D_{31}^\lambda(\mathbf{k})\pm i\sigma D_{32}^\lambda(\mathbf{k})]\big\}(\phi_{n+1,s}^{-\sigma}-\phi_{n-1,s}^{-\sigma})\\ &-(e/2\Omega)^2[D_{21}^\lambda(\mathbf{k})\pm i\sigma D_{22}^\lambda(\mathbf{k})](\phi_{n+2,s}^{-\sigma}+\phi_{n-2,s}^{-\sigma}) - i(e/2\Omega)^3[D_{31}^\lambda(\mathbf{k})\pm i\sigma D_{32}^\lambda(\mathbf{k})](\phi_{n+3,s}^{-\sigma}-\phi_{n-3,s}^{-\sigma}) = 0\ , \quad (7)\end{aligned}$$

where

$$\begin{aligned}
D_{01}^{HH} &= \gamma_a^{HH}k_y^3+\gamma_b^{HH}k_x^2k_y\ , & D_{02}^{HH} &= \gamma_a^{HH}k_x^3+\gamma_b^{HH}k_y^2k_x\ ,\\
D_{01}^{LH} &= \gamma_a^{LH}k_y^3+\gamma_b^{LH}k_x^2k_y+\gamma_c^{LH}\langle k_z^2\rangle k_y\ , & D_{02}^{LH} &= \gamma_a^{LH}k_x^3+\gamma_b^{LH}k_y^2k_x+\gamma_c^{LH}\langle k_z^2\rangle k_x\ ,\\
D_{11}^{HH} &= 3\gamma_a^{HH}k_y^2E_y+\gamma_b^{HH}(k_x^2E_y+2k_xk_yE_x)\ , & D_{12}^{HH} &= 3\gamma_a^{HH}k_x^2E_x+\gamma_b^{HH}(k_y^2E_x+2k_yk_xE_y)\ ,\\
D_{11}^{LH} &= 3\gamma_a^{LH}k_y^2E_y+\gamma_b^{LH}(k_x^2E_y+2k_xk_yE_x)+\gamma_c^{LH}\langle k_z^2\rangle E_y\ , & D_{22}^{\lambda} &= 3\gamma_a^{\lambda}k_xE_x^2+\gamma_b^{\lambda}(2k_yE_xE_y+k_xE_y^2)\ ,\\
D_{21}^{\lambda} &= 3\gamma_a^{\lambda}k_yE_y^2+\gamma_b^{\lambda}(2k_xE_yE_x+k_yE_x^2)\ , & D_{12}^{LH} &= 3\gamma_a^{LH}k_x^2E_x+\gamma_b^{LH}(k_y^2E_x+2k_yk_xE_y)+\gamma_c^{LH}\langle k_z^2\rangle E_x\ ,\\
D_{31}^{\lambda} &= \gamma_a^{\lambda}E_y^3+\gamma_b^{\lambda}E_x^2E_y\ , & D_{32}^{\lambda} &= \gamma_a^{\lambda}E_x^3+\gamma_b^{\lambda}E_y^2E_x\ .
\end{aligned}$$

All eigenvalues can be written as $q_{s,n}=q_{s,0}+n\Omega$ where $q_{s,0}$ is the eigenvalue in the region $(-\Omega/2,\Omega/2]$. It is evident that $q_{s,n}$ and $q_{s,0}$ are physically equivalent. We also find $s=+$ branch and $s=-$ branch satisfying the relations:

$$\phi_{n,-}^\sigma = -\sigma\phi_{-n,+}^{-\sigma,*}\ , \quad (8)$$

$$q_-(\mathbf{k}) = -q_+(\mathbf{k})\ . \quad (9)$$

With the help of Green function, we can calculate the density of states (DOS) $\rho_{\sigma,\sigma}$ and the density of spin polarization(DOSP) $\rho_{\sigma,-\sigma}$,[3,9]

$$\begin{aligned}\rho_{\sigma_1,\sigma_2}(T,\omega) &= \frac{1}{2\pi}\int_{-\infty}^{\infty}d\mathbf{k}\sum_{s=\pm}\sum_{\substack{l_1,l_2\\n,m=-\infty}}^{\infty}e^{i(n-m)\Omega T}\\ &\times R_{\sigma_1,\sigma_2}(s;n,m;\mathbf{k})J_{l_1}(-2b_0\mathbf{k}\cdot\mathbf{E}\sin(\Omega T))\\ &\times J_{l_2}(2\gamma\cos(2\Omega T))\delta(\omega-[E_{\mathbf{k}}+E_{em}\\ &-(l_1+2l_2+n+m)\Omega/2+q_s(\mathbf{k})])\ , \quad (10)\end{aligned}$$

in which $J_n(x)$ is the Bessel function of nth order, $R_{\sigma_1,\sigma_2}(s;n,m;\mathbf{k}) = (\eta_{\sigma_1}{}^\dagger\phi_{n,s}(\mathbf{k}))(\phi_{m,s}{}^\dagger(\mathbf{k})\eta_{\sigma_2})$ with η_σ standing for the eigenfunction of σ_z. It is seen from Eq. (10) that these densities are periodic functions of T with period T_0. The DOSP is nonzero only when both the RF and the SOC are present. Furthermore, the induced magnetic moment can be written as

$$\begin{aligned}\mathbf{M}(T) &= \Big(M_x(T),M_y(T),M_z(T)\Big)\\ &= \frac{2g\mu_B}{n_\uparrow+n_\downarrow}\int_{-\infty}^{E_F(T)}d\omega\Big(\mathrm{Re}\,\rho_{\uparrow,\downarrow},-\mathrm{Im}\,\rho_{\uparrow,\downarrow},\\ &\frac{1}{2}(\rho_{\uparrow,\uparrow}-\rho_{\downarrow,\downarrow})\Big)\ , \quad (11)\end{aligned}$$

where the Fermi energy $E_F(T)$ is determined by $n_\sigma = \int_{-\infty}^{E_F(T)}\rho_{\sigma,\sigma}(\omega,T)\,d\omega$ where n_σ represents the hole concentration. Eq. (11) has been simplified by using the fact that $\rho_{\sigma_1,\sigma_2}=\rho_{\sigma_2,\sigma_1}^*$. It is evident that $E_F(T)$ and $\mathbf{M}(T)$ both oscillate with the period T_0. Due to time reversal symmetry, the DOSP is an odd function of the time $\rho_{\sigma,-\sigma}(T,\omega) = -\rho_{\sigma,-\sigma}(-T,\omega)$, and therefore the DOSP averaged over time reduces to zero. Besides, the DOS is an even function $\rho_{\sigma,\sigma}(T,\omega)=\rho_{\sigma,\sigma}(-T,\omega)$ and $\rho_{\uparrow,\uparrow}(T,\omega)=\rho_{\downarrow,\downarrow}(T,\omega)$, thus the RF in the x-y plane cannot induce magnetic moment along the z axis. These characters are similar to those of a 2DEG.[9]

We numerically solve the eigen-equation Eq. (7) and calculate the DOS and the DOSP through Eq. (10). One can further obtain the magnetic moment by using Eq. (11). In the calculation we choose $a=10$ nm, $E_z=30$ kV/cm. The material parameters of GaAs are as follows:[13,18] $\gamma_1=6.85$, $\gamma_2=2.1$, $\gamma_3=2.9$, $\Delta_0=0.341$ eV, $g_{LH}=1.2$, $g_{HH}=3.6$, $m_{LH}^*=0.0537\ m_0$ and

$m^*_{HH} = 0.171\ m_0$. In order to ensure the validity of the model which we adopt, we must keep the highest sideband of HH well separated from the lowest sideband of LH. Moreover, the HH and LH bands can be splitted by 50 meV by adjusting the applied strain.[5] According to these, we choose $E = 0.1$ kV/cm, $\Omega = 0.1$ THz in the following calculation.

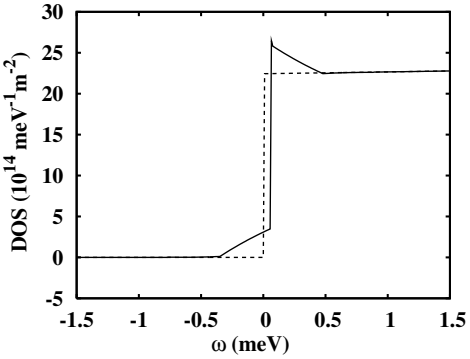

FIG. 1: Time-averaged DOS of HHs under THz field with $E = 0.1$ kV/cm, $\Omega = 0.1$ THz (solid curve) and without THz field (dashed curve).

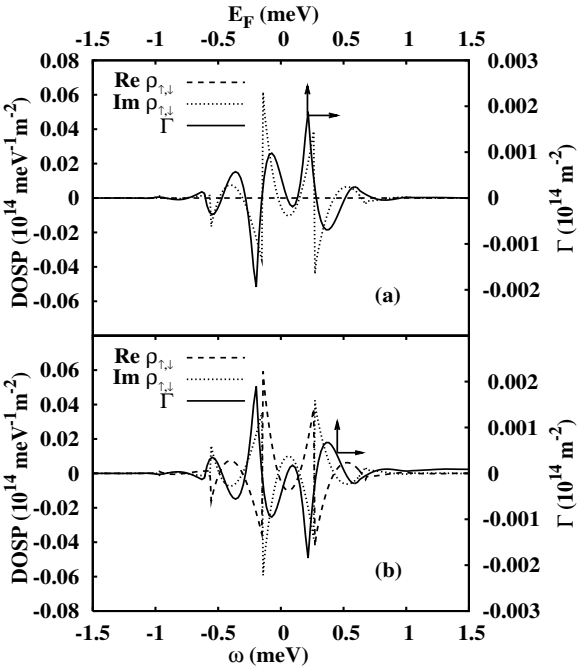

FIG. 2: DOSP of HHs for (a) $\theta_E = 0$ and (b) $\theta_E = \pi/4$ at $T = T_0/4$ with $E = 0.1$ kV/cm, $\Omega = 0.1$ THz. The real part and imaginary part are plotted as dashed curves and dotted curves respectively. The solid curves is Γ as a function of E_F. Note the scale of E_F and Γ are on the upper and right frame of the figure.

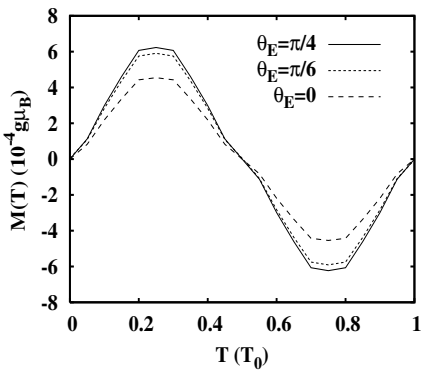

FIG. 3: Magnetic moment M of HHs versus time for $\theta_E = 0$, $\theta_E = \pi/6$ and $\theta_E = \pi/4$ with $E = 0.1$ kV/cm, $\Omega = 0.1$ THz. The concentration of HH is $n_\uparrow = n_\downarrow = 0.7 \times 10^{11}$ cm^{-2} and E_F is about 0.35 meV.

In Fig. 1 we compare the time-averaged DOS with and without the THz field. Due to DFKE, the main absorption edge has a blueshift and the DOS becomes finite below the band gap. The DOSP at $T = T_0/4$ are plotted in Fig. 2 for THz field along two different directions, (a) $\theta_E = 0$ and (b) $\theta_E = \pi/4$. It is seen from Fig. 2(a) that only the imaginary part of DOSP is finite. From Eq. (11), we can find that the induced magnetic moment is along the y axis. This is similar to the 2DEG case with Rashba SOC.[9] In Fig. 2(b), we can see that $\mathrm{Re}\,\rho_{\uparrow,\downarrow} = -\mathrm{Im}\,\rho_{\uparrow,\downarrow}$. Thus the induced magnetic moment is along the $(1,1,0)/\sqrt{2}$ direction, i.e., parallel to the THz field. These results indicate that the direction of the induced magnetic moment varies with that of the THz field, which is different from the 2DEG case with Rashba SOC.[9] This is due to the anisotropy of the SOC Hamiltonian.

In Fig. 3, the magnetic moment of M is plotted as function of time for $\theta_E = 0$, $\theta_E = \pi/6$ and $\theta_E = \pi/4$ with $E = 0.1$ kV/cm, $\Omega = 0.1$ THz. It is noted that that the magnitude of magnetic moment depends on the direction of the THz field θ_E. The magnetic moment is the smallest for $\theta_E = 0$ and the largest for $\theta_E = \pi/4$.

In Fig. 2, we also plotted Γ as function of E_F, where $\Gamma = \int_{-\infty}^{E_F} \mathrm{Im}\,\rho_{\uparrow,\downarrow}\, d\omega$. It is noted that Γ is very small for large enough E_F, hence M becomes negligible when the concentration of the hole gas is high. This can be understood as follows: By interchanging the order of integral, one has

$$\begin{aligned}\int_{-\infty}^{\infty} \rho_{\uparrow,\downarrow}\, d\omega \;=\; & \int_{-\infty}^{\infty} d\mathbf{k} \sum_{l_1} J_{l_1}(-2b_0\mathbf{k}\cdot\mathbf{E}\sin(\Omega T)) \\ & \times \sum_{s,m,n} R_{\uparrow,\downarrow}(s;n,m;\mathbf{k}) e^{i(n-m)\Omega T} \\ & \times \sum_{l_2} J_{l_2}(2\gamma\cos(2\Omega T))\ .\end{aligned}$$

By virtue of Eqs. (8) and (9), one gets $R_{\uparrow,\downarrow}(s;n,m;\mathbf{k}) =$

$-R_{\uparrow,\downarrow}(-s;-m,-n;\mathbf{k})$. Thus the terms of $s=+$ branch compensate those of $s=-$ branch, and the integral of the DOSP over the whole range $(-\infty,\infty)$ is zero. On the other hand, the DOSP decays to very small value with increasing ω due to the interference caused by the momentum dependence of the SOC. Hence the contribution to the magnetic moment at large ω is negligible. Accordingly, M becomes very small when E_F is large, i.e., the hole concentration is high. Our calculation shows that this is also true for 2DEG with Rashba SOC.

In conclusion, we study the effects of the intense THz field on 2DHG with Rashba SOC. We calculate the DOS and DOSP. We also show that the a THz magnetic moment can be excited for low hole concentration. It is noted that the direction of the THz field has a strong influence on the angle between the induced magnetic moment and the THz field, as well as on the amplitude of the magnetic moment, which is quite different from 2DEG with Rashba SOC case. We also point out that the magnetic moment becomes very small if the hole concentration is high enough, due to the interference caused by the momentum dependence of the SOC. This effect also appears in 2DEG.

The author would like to thank M. W. Wu for proposing the topic as well as the directions during the investigation. This work was supported by the National Natural Science Foundation of China under Grant No. 10574120, the National Basic Research Program of China under Grant No. 2006CB922005, the Knowledge Innovation Project of Chinese Academy of Sciences and SRFDP. The author would also like to thank J. H. Jiang for helpful discussions and I. C. da Cunha Lima for proof reading of this manuscript.

[1] W. Franz, Z. Naturforsch. Teil A **13**, 481 (1958).
[2] L. V. Keldysh, Sov. Phys. JETP **34**, 788 (1958).
[3] A. P. Jauho and K. Johnsen, Phys. Rev. Lett. **76**, 4576 (1996).
[4] K. Johnsen and A. P. Jauho, Phys. Rev. B **57**, 8860 (1998).
[5] K. B. Nordstrom, K. Johnsen, S. J. Allen, A. -P. Jauho, B. Birnir, J. Kono, and T. Noda, Phys. Rev. Lett. **81**, 457 (1998).
[6] J. Cerne, K. Kono, T. Inoshita, M. Sundaram, and A. C. Gossard, Appl. Phys. Lett. **70**, 3543 (1997).
[7] J. Kono, M. Y. Su, T. Inoshita, T. Noda, M. S. Sherwin, S. J. Allen, Jr., and H. Sakaki, Phys. Rev. Lett. **79**, 1758 (1997).
[8] C. Phillips, M. Y. Su, M. S. Sherwin, J. Ko, and L. Coldren, Appl. Phys. Lett. **75**, 2728 (1999).
[9] J. L. Cheng and M. W. Wu, Appl. Phys. Lett. **86**, 032107 (2005).
[10] J. H. Jiang, M. Q. Weng, and M. W. Wu, J. Appl. Phys. **100**, 063709 (2006).
[11] J. H. Jiang and M. W. Wu, Phys. Rev. B **75**, 035307 (2007).
[12] Y. A. Bychkov and E. Rashba, Sov. Phys. JETP Lett. **39**, 78 (1984).
[13] R. Winkler, *Spin-Orbit Coupling Effects in Two-Dimensional Electron and Hole Systems* (Springer, Berlin, 2003).
[14] C. Lü, J. L. Cheng, and M. W. Wu, Phys. Rev. B **73**, 125314 (2006); *ibid.* **71**, 075308 (2005).
[15] J. Luo, H. Munekata, F. F. Fang, and P. J. Stiles, Phys. Rev. B **41**, 7685 (1990).
[16] J. Nitta, T. Akazaki, H. Takayanagi, and T. Enoki, Phys. Rev. Lett. **78**, 1335 (1997).
[17] J. H. Shirley, Phys. Rev. **138**, B979 (1965).
[18] *Numerial Data and Functional Relationships in Science and Technology*, Landolt-Börnstein, New Series Vol. 17, edited by O. Madelung, M. Schultz, and H. Weiss (Springer, Berlin, 1982).